Polymer 118 (2017) 68–74

Contents lists available at ScienceDirect

Polymer

journal homepage: www.elsevier.com/locate/polymer

Synthesis and characterization of polypropylene/iron encapsulated carbon nanotube composites with high magnetic response at room temperature

Muhammad Nisar [a], Carlos Pérez Bergmann [b], Julian Geshev [c], Raúl Quijada [d], Griselda Barrera Galland [a, *]

[a] Instituto de Química, Universidade Federal do Rio Grande do Sul, Av. Bento Gonçalves 9500, 91501-970 Porto Alegre, Brazil
[b] Laboratório de Materiais Cerâmicos, Departamento de Materiais, Universidade Federal do Rio Grande do Sul, Porto Alegre, Brazil
[c] Instituto de Física, Universidade Federal do Rio Grande do Sul, Porto Alegre, Brazil
[d] Departamento de Ingeniería Química y Biotecnología, Facultad de Ciencias Físicas y Matemáticas, Universidad de Chile, Santiago, Chile

ARTICLE INFO

Article history:
Received 15 February 2017
Received in revised form
18 April 2017
Accepted 19 April 2017
Available online 27 April 2017

Keywords:
Polypropylene
Carbon nanotube
Magnetic nanocomposites

ABSTRACT

Magnetic and conducting polypropylene (PP) polymer nanocomposites with different loadings of synthetic carbon nanotubes (CNT-Fe) were fabricated by *in-situ* polymerization. Chemical vapor deposition was used as the synthetic route for carbon nanotube (CNT) synthesis, in which high-surface-area silica (SiO_2) acts as the support and ferrocene as the precursor and catalyst. Scanning and transmission electron microscopy analyses evidence the homogenous dispersion of the filler in the polymer matrix. It was found that, with the addition of 3.8 wt.% of the filler, the insulating PP matrix changes to a semiconductor. The magnetic properties of the nanocomposites were investigated using a vibrating sample magnetometer. The addition of 0.8 wt.% CNTs results in ferromagnetic behavior in the diamagnetic polymer matrix and high coercivities at room temperature. The thermal properties were investigated by thermogravimetric analysis and differential scanning calorimetry. Results show an increase in the maximum degradation, crystallization, and melting temperatures of the nanocomposites as compared with neat PP.

1. Introduction

Inorganic–organic composite materials are becoming increasing important because of their remarkable properties, which can be attributed to the synergism between the properties of their components. There are several routes to prepare these materials, with the most important one perhaps being the incorporation of inorganic components in organic polymers. These materials have attracted the attention of the researchers owing to the significant changes in their mechanical, thermal, electrical, and magnetic properties, compared to pure organic polymers [1]. Polymer nanocomposites demonstrate remarkable enhancement in some properties with a very low amount of addition of fillers such as exfoliated nanosilicate layers, carbon nanotubes (CNTs), and graphite nanoplatelets. However, for the effective performance of these fillers, the strong interfacial adhesion between the nanofiller and polymer matrix and the homogenous dispersion of the filler in the polymer matrix are imperative [2].

The discovery of carbon nanotubes in 1991 by Iijima [3] has opened a new area of research on the structure, properties and applications of this unique material. In 1994, the first polymeric nanocomposite using CNTs as the filler was reported by Ajayan et al. [4] The exceptional combination of the mechanical, electrical, and thermal properties of the CNTs make them excellent candidates to alternate or balance the conventional nanofillers in the manufacture of multifunctional polymer nanocomposites [5]. The reinforcing behavior of CNTs in a polymer matrix has also generated a lot of research interest in the past two decades [6]. However, to confer the special properties of CNTs to the polymer matrix, the uniform dispersion of CNTs in the polymer matrix is required, which is difficult. The delocalization of π electrons, small size of CNTs, and large surface area result in van der Waals forces, which cause aggregation [7,8]. However, some researchers have demonstrated uniform distribution of the filler using *in situ*

* Corresponding author.
E-mail address: griselda.barrera@ufrgs.br (G.B. Galland).

http://dx.doi.org/10.1016/j.polymer.2017.04.067
0032-3861/

polymerization [9–12].

Polypropylene (PP) is one of principal polyolefin's with commercial importance because of its cost-effectiveness and intrinsic properties, such as low density, high stiffness, good tensile strength, and inertness toward acids, alkalis, and solvents. PP has been used in many industrial applications, such as packaging materials, textiles, and automotive parts. However, for advanced applications, the physicochemical properties of PP need to be further improved or new functionalities must be introduced [13]. In order to improve the dispersion of CNTs in a polymer matrix, various methods have been employed. Common methods for CNT-filled polymer nanocomposites include melt blending [14–16], solution mixing [17], and *in situ* polymerization [18]. The limitation of the melt blending method is that it does not always yield homogenous dispersion of the nanotubes because of the lack of compatibility [19]. In the case of PP and PE, the use of the solution mixing method becomes impossible since these polymers are soluble in solvents such as xylene and trichlorobenzene above 120 °C, which have considerable health risks [2]. The *in situ* polymerization is the most suitable technique used to achieve uniform dispersion of the filler, when compared to the conventional melt mixing [20].

Both academic and industrial researchers have been paying increased attention to magnetic polymer nanocomposites. Magnetic nanoparticles and nanocomposites have attracted significant scientific and technological interest because of their potential application in the fields of biomedicine, information technology, magnetic resonance imaging, catalysis, telecommunication, and environmental remediation [21–23]. In contrast, magnetic nanoparticles similar to conventional CNTs tend to aggregate in a polymer matrix and reduce the energy associated with high surface area of the nanosized particles [24]. Iron is the conventionally most-used magnetic material [25] and its excellent magnetic performance has recently attracted considerable interest. However, iron nanoparticles have significant disadvantages such as easy oxidation, which must be resolved when using iron NPs as the filler. Some researchers have reported that the encapsulation of magnetic NP in CNTs can resolve this difficulty [26,27]. Bhatia et al. [28] reported the synthesis of multiwall carbon nanotubes by chemical vapor deposition using ferrocene [$Fe(C_2H_5)_2$], an organometallic compound, which acts as both a catalyst and precursor of synthesis and does not require high temperature. Recently, Osorio et al. [29,30] used silica different surface areas as the substrate and ferrocene as the precursor, and optimized the conditions for the CNTs synthesis. They reported that variation in the temperature and dwell time of the synthesis can help tune the final magnetic properties, i.e., the composition of the iron-containing phases in the CNTs.

Our research group is extensively working on synthesizing polyolefin nanocomposites using *in situ* polymerization. Recently, we prepared polyethylene–graphite nanosheet (PE-GNS), isotactic polypropylene–graphite nanosheet (iPP-GNS) nanocomposites, and polyethylene-CNTs-Fe nanocomposites and obtained homogenous dispersions of the filler in the polymer matrix [31–37]. Park et al. [38] reported the synthesis of polypyrrole (PPy)-coated magnetite (Fe_3O_4) hybrid particles of dual stimuli-response under magnetic and electric fields. The aim of the present work is to prepare nanocomposites of polypropylene iron-encapsulated carbon nanotubes (PP-CNT-Fe) through *in situ* polymerization using metallocenes [rac-Ethylene bis (indenyl) Zirconium (*rac*-$Et(Ind)_2ZrCl_2$)] as a catalyst and methylaluminoxane (MAO) as a co-catalyst in order to obtain a dual stimuli responsive material under electric and magnetic fields. This multifunctional material has the potential to be applied as sensors in medicine and in electronic devices, low-temperature heaters, energy storage devices [39], solar cells, magnetic recording materials [40], magnetic sensors, [41] and microwave absorbers [42], in the aerospace and automotive industries.

2. Experimental

2.1. Materials

The metallocene catalyst *rac*-ethylenebis (indenyl) Zirconium (*rac*-$Et(Ind)_2ZrCl_2$) (Aldrich) was used as the propene polymerization catalyst and MAO (Chemtura, 10 wt% Al solution in toluene) as the cocatalyst. Metallic sodium and benzophenone were used for the distillation of toluene, which was used as solvent. The deoxygenating and drying process of propylene was carried out by passage through the columns of Cu catalyst (BASF) and activated molecular sieves (13X). All manipulates were carried out in inert nitrogen atmosphere using standard Schlenk techniques.

2.2. Carbon nanotube synthesis

The CNTs containing iron (CNT-Fe) were synthesized by chemical vapor deposition (CVD), using the method reported in Refs. [29,30]. Ferrocene was used as a precursor and high-surface-area silica as a support. The reaction time was approximately 2 min, and the temperature was increased up to 750 °C.

2.3. Polymerization reactions

The CNTs-Fe were stirred with 15 wt.% of MAO for 30 min in toluene. The polymerization reactions were carried out in a Buchi glass reactor of 1 L capacity equipped with a mechanical stirrer and thermocouple. First, toluene was introduced as a solvent, and previously treated CNTs-Fe with MAO were used as the filler, followed by addition of the co-catalyst (MAO, Al/Zr = 1000). Subsequently, the system was saturated with propylene gas and, finally, a given aliquot of catalyst [(*rac*-$Et(Ind)_2ZrCl_2$) (5.0×10^{-6} mol)] solution in toluene was introduced. The reaction was carried out at 25 °C under 2 bar pressure of propylene, with a stirring rate of 1000 rpm for 30 min. The reaction was terminated with the addition of 5% by volume HCl/methanol 10 vol% solution. Finally, the polymer was precipitated with methanol, filtered and washed before dry to constant weight.

2.4. Characterization of polymer nanocomposites

Transmission electron microscopy (TEM) analyses were performed using a JEOL 1011 microscope operating at 120 kV. Copper grid of 300 mesh covered with amorphous carbon was used for sample preparation. A drop of the solution was deposited on the copper grid or from ultrathin films (~50 nm) cut under cryogenic conditions with a Leica Ultracut UCT microtome at −70 °C and placed on a grid (polymeric nanocomposites).A Phillips XL30microscope operating at 20 kV was used for scanning electron microscopy (SEM). Samples were deposited on an aluminum stub and coated with gold.

The molecular weight analyses were carried out using a Waters Alliance GPC 2000 instrument operating with three Styragel HT-type columns (HT3, HT5, and HT6E). At a temperature of 135 °C and 1,2,4-trichlorobenzene with a flow rate of 1 ml/min was used as a solvent. Polystyrene was used as the column calibration standard.

The Fe on the carbon nanotubes was determined by HR-CS GF AAS through direct solid sampling (SS) using a contrAA 700 high-resolution continuum source atomic absorption spectrometer (Analytik Jena AG, Jena, Germany). The samples were directly weighed, without any prior preparation step, on pyrolytically coated graphite tubes. A pre-adjusted pair of tweezers, which is

part of the SSA 6 manual solid sampling accessory (Analytik Jena), was used to transfer the platforms to the atomizer. The program temperatures and methods used were followed and adapted from the literature. [43] A 10 μL volume of a mixture of 20 μg Pd + 12 μg Mg was used as the chemical modifier dosed onto the sample prior to platform introduction into the atomizer. Pyrolysis and atomization temperatures were 800 °C and 2500 °C, respectively, using the 283.245 nm line and only the central pixel for evaluation.

The electrical resistivity was measured with the help of a megohmmeter (Megger BM11) operating at the highest voltage of 1200 V. With this set-up, the standard two-point method was used. For each electrical value displayed in this contribution, at least four samples were prepared, and four measurements were taken for each sample. In general, differences of around one order of magnitude were detected in the non-percolated samples having low conductivity values (~10^{-9} S/cm). For percolated samples, the experimental error for conductivities was less than 50%. The samples prepared to use for the test were 40 mm × 15 mm in size and 1 mm in thickness.

The magnetic properties of the CNTs and nanocomposites were investigated by using an EZ9MicroSense vibrating sample magnetometer (VSM) at room temperature with a magnetic field (H) cycled between−20 kOe and +20 kOe.

The thermal properties were measured by differential scanning calorimetry (DSC) using a Perkin–Elmer differential calorimeter (model DSC Q20); the temperature was increase from 0 to 180 °C with a heat rate of 10 °C/min. The second scan was used to determine the melting temperature T_m, and the percent crystallinities were calculated from the enthalpy of fusion data obtained from the DSC curves (207 J/g was used for 100% crystalline material). Thermogravimetric analysis (TGA)/SDT Q600 thermal analyzer Q20 (TA Instruments) was used to determine the thermal stability of the nanocomposites with respect to the neat polymer. The samples were scanned in the range of 0–800 °C, at a scanning rate of 20 °C/min.

3. Results and discussion

3.1. Polymerization

Propylene polymerizations were carried out in the presence of iron encapsulated in carbon nanotubes (CNTs-Fe) using metallocene (*rac*-Et(Ind)$_2$ZrCl$_2$) as a catalyst and methylaluminoxane (MAO) as a cocatalyst. The CNT-Fe was first stirred with 15 wt% of MAO for 20 min to remove the impurities. Table 1 presents the results of a series of polymerization reactions performed with different percentages of CNT-Fe. The filler concentration in the PP/CNT-Fe nanocomposites ranged from 0.8 to 7.5 wt.%, as calculated from the polymer yield. It can be seen that the catalytic activity decrease up to 43% with the incorporation of 0.8% of the filler; in contrast, the amount of filler does not significantly affect the catalytic activities. In spite of this decrease, the catalytic activities still remain very high.

3.2. Thermal properties

Table 1 also shows the thermal properties of PP and its nanocomposites. The melting temperatures of the nanocomposites (141–144 °C) show an increase of 3 °C as compared with the neat PP. Similarly, the crystallization temperature (T_c) shows an increase of 9–11 °C for all the nanocomposites, indicating that the filler acts as a nucleating agent for PP. Interestingly, the nucleation effect gradually shifts to higher temperatures as the filler content increases; in other words, addition of higher amount of filler produces large heterogeneous nucleation effect. Similar effect has been found by other researchers for PP/MWNT and PP/SWNT [44,45]. The percentage crystallinity values gradually increased with increasing filler amount.

The thermal degradation behavior of neat PP and PP/CNT-Fe nanocomposites has been investigated by TGA analysis. It can be seen from Table 1 that, with the incorporation of the filler, the maximum (T_{max}) and the initial (T_{onset}) degradation temperatures increased by 9 and 26 °C, respectively. It can be noted that, at a low concentration of the filler (<1 wt.%), T_{max} decreases by approximately 3 °C, whereas T_{onset} remains almost constant. This is attributed to the presence of Fe, which acts as a catalyst for degradation; such a catalytic effect of Fe has been shown in a previous work with polyethylene/CNT-Fe nanocomposites [37]; for nanocomposites containing up to 3.8 wt.% of CNT-Fe, the catalytic activity of Fe is not significant. The explanation is that the thermal stabilizing effect is mostly attributed to the formation and stabilization of CNT-bonded macroradicals [46] and the nanotube barrier effect [47]. In contrast, the decrease in T_{max} and T_{onset} with the highest amount of filler (7.5 wt.%) is probably due to the presence of the higher percentage of Fe in the nanocomposites (see Table 2), which is twice the amount of Fe present in the nanocomposite with 3.8 wt.% CNT-Fe. This can compensate for the stabilization of CNTs and potentiate the catalytic effect of Fe towards degradation [45]. The TGA residue weight percentage (wt.%) at 500 °C is in close agreement with the amount of filler calculated from the polymer yield. These results confirm that a good distribution of the filler is achieved in the nanocomposites.

3.3. Effect of polymerization temperature on the molecular weight

The effect of the polymerization temperature on the molecular weight of the polymer was also studied. It was confirmed from the GPC results that the polymerization at 25 °C produces a polymer of comparatively higher molecular weight (4.4 × 10^4 g mol^{-1} with polydispersity of 1.9), whereas the polymerization that takes place at 60 °C produces a polymer of lower molecular weight (1.9 × 10^4 g mol^{-1} with polydispersity of 1.8). The previous results showed that the nanocomposites retain the same molecular weight

Table 1
Results of nanocomposites of polypropylene with different amounts of CNT-Fe.

Samples	Filler (%)	Polymer (g)	TGA residue (%)	Catalytic activity[a]	T_c(°C)	T_m (°C)	Xc(%)	T_{onset}(°C)	T_{max}(°C)
PP	0	40.8	0.95	8163	105	141	56	425	476
PP/CNT$_{Fe1}$	0.8	23.9	1.44	4709	114	143	57	426	473
PP/CNT$_{Fe2}$	2.3	17.18	2.38	3437	114	143	58	442	482
PP/CNT$_{Fe3}$	3.0	18.0	2.51	3602	114	143	62	451	483
PP/CNT$_{Fe4}$	3.8	18.5	2.44	3706	116	144	62	452	485
PP/CNT$_{Fe5}$	7.5	18.60	5.50	3713	116	144	57	415	483

[a] KgPE.[Zr]$^{-1}$.h^{-1}.bar^{-1}.

Table 2
Iron content, conductivity, saturation magnetization (M_S), normalized remnant magnetization (M_R/M_S), and coercivity (H_C) values of the nanocomposites of polypropylene with different amounts of CNT-Fe.

Sample	Filler (%)	Fe[a] (wt.%)	Conductivity (S cm^{-1})	M_S (emu/g)	M_R/M_S	H_C(Oe)
PP	–	0	6.5×10^{-11}	–	–	–
CNT-Fe	–	26.9	–	13.1(±1.0)	0.32(±0.1)	280(±5)
PP/CNT$_{Fe1}$	0.8	0.23	6.3×10^{-11}	17.9(±1.0)	0.33(±0.1)	420(±5)
PP/CNT$_{Fe2}$	2.3	0.63	6.9×10^{-11}	14.0(±1.0)	0.34(±0.1)	430(±5)
PP/CNT$_{Fe3}$	3.0	0.89	6.4×10^{-11}	11.3(±1.0)	0.37(±0.1)	530(±5)
PP/CNT$_{Fe4}$	3.8	1.02	7.8×10^{-5}	11.6(±1.0)	0.40(±0.1)	710(±5)
PP/CNT$_{Fe5}$	7.5	2.03	1.3×10^{-4}	16.0(±1.0)	0.34(±0.1)	450(±5)

[a] Fe,From Atomic Absorption.

as that of the neat polymer when using the same route for the study of the nanocomposites [33].

3.4. Morphology of the nanocomposites

SEM and TEM studies were carried out to observe the morphology and dispersion of the filler in the polymer matrix. Fig. 1 shows the SEM images of the neat PP and PP/CNT-Fe nanocomposites at the same magnification. It can be seen that the polymer is coated around the CNTs, clearly showing that the filler is uniformly distributed in the polymer matrix; no agglomerates were observed.

The CNT-Fe obtained by the method used in this work are a mixture of single and multiwall CNTs with various lengths [29,30]. Fig. 2 shows the TEM micrographs of PP nanocomposites with 0.8 wt.% (A), (B), and (C), and 7.5 wt.% (D), (E), and (F) of CNT-Fe, respectively, at different magnifications. The black spots observed in the figures are the Fe nanoparticles. It is clear from the images that CNTs are uniformly distributed in the PP matrix, and no aggregation was observed. At higher magnifications, for example 100 nm, the isolated CNTs can be clearly seen encapsulating Fe.

3.5. Conductive and magnetic behavior of the nanocomposites

One of the objectives of this work was to transform an insulating material to a semiconductor. A significant concentration of conductive filler, beyond the electrical percolation threshold, is mandatory to create a conductive network in the insulator polymer matrix. This decreases the electrical resistivity of the material immediately by several orders of magnitude. The aspect ratio and dispersion of the conductive nanofillers are the two major factors considered while taking into account the electrical percolation threshold [48]. The values of the electrical conductivity of PP and its nanocomposites are listed in Table 2 and plotted in Fig. 3. The conductivity of the neat PP is practically zero (6.5×10^{-11} S cm^{-1}) as expected, which matches the insulation nature of the material. It can be seen that, with the addition of only 3.8 wt.% CNT-Fe, the conductivity sharply raises to a value of 7.8×10^{-5} S cm^{-1}, and reaches a higher value of 1.3×10^{-4} S cm^{-1} with the addition of 7.5 wt.% of the filler. In our previous work, we obtained PE/CNT-Fe nanocomposites with good magnetic properties, and when the measurements were carried out after a 6-month interval, the same results were obtained confirming that the Fe is protected from oxidation since no losses in the magnetic properties were observed. However, the amount of the filler was not enough (2.5 wt.%) to transform the insulating PE to a semiconductor [37]. Fig. 3 clearly shows that the percolation threshold is between 3.0 and 3.8 wt.% of CNT-Fe in PP.

Magnetization hysteresis loops of the CNT-Fe powder and two representative PP/CNT-Fe nanocomposites, measured at room temperature, are plotted in Fig. 4(a) and (b), respectively; the PP alone (not shown) shows evidence of only a diamagnetic signal. The characteristics of the hysteresis loops change significantly as the magnetic filler content is varied; initially, both the remnant

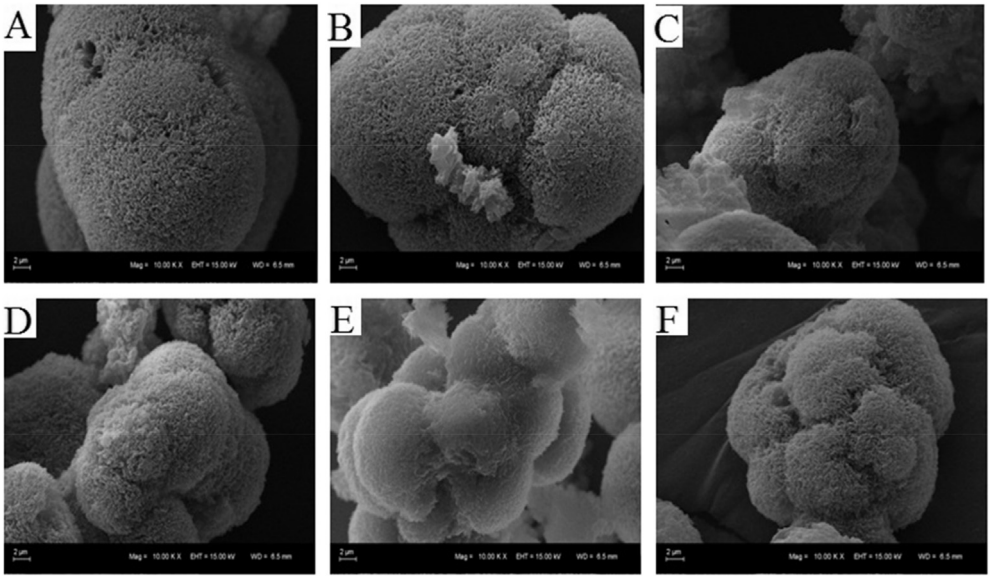

Fig. 1. SEM images of the (A) neat PP, (B) 0.8 wt. %, (C) 2.3 wt. %, (D) 3 wt.%, (E) 3.8 wt.%, and (F) 7.5 wt.% of CNT-Fe in PP.

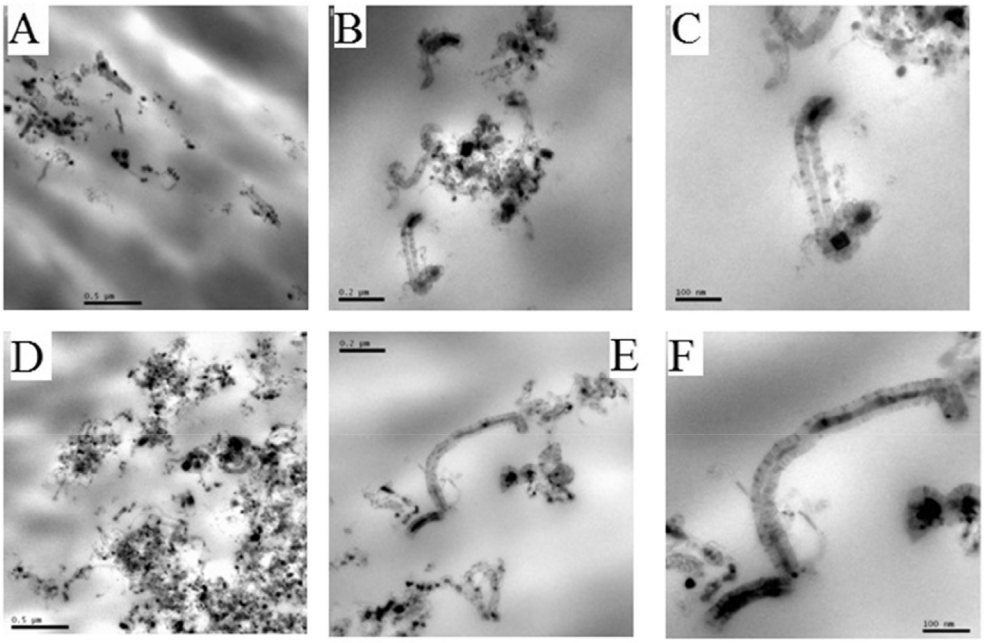

Fig. 2. TEM Images of 0.8 wt.% PP/CNT-Fe nanocomposites (A), (B), and (C) and 7.5 wt.% PP/CNT-Fe nanocomposites (D), (E), and (F).

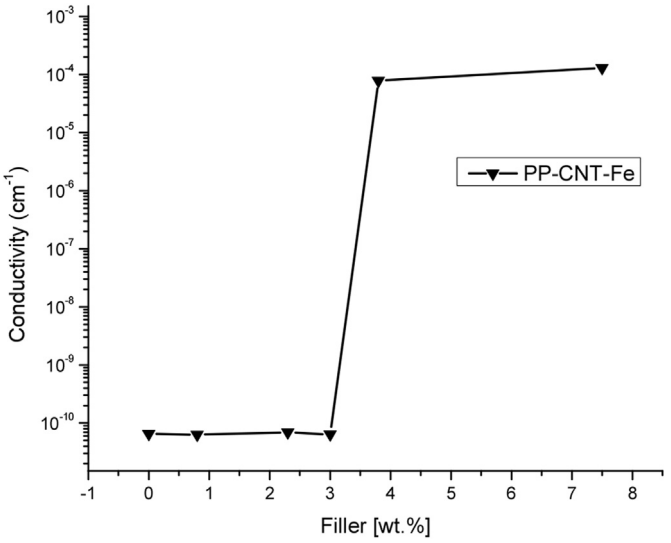

Fig. 3. Effect of the filler on the electrical conductivity of the polypropylene nanocomposites.

magnetization/saturation magnetization ratio (M_R/M_S) and the coercivity (H_C) increase sharply as the filler increases up to ~4 wt.%, as shown in Fig. 4(d) and (e), while M_S (plotted in Fig. 4(c)) shows a variation quite opposed to those of M_R/M_S and H_C. Fang et al. [49] reported a reduction of 12.8% in the saturation magnetization for the PANI coated carbonyl iron (CI) particles compared with pure CI. The magnitudes of the M_R/M_S and H_C of the samples with the highest filler content studied here, namely 7.5 wt.%, drop significantly, having values approximately equal to those of the PP/CNT-Fe nanocomposite with filler of 2.3 wt.%. The values of M_S, M_R/M_S, and H_C of all nanocomposites are given in Table 2. He *et al.* [50] showed a similar decreasing trend for high-density polyethylene (HDPE) matrix in H_C; as the percentage of the magnetic constituent increased from 5 to 20 wt.%, the value of H_C decreased quickly from 193 to 9 Oe. This much lower value of H_C for higher amount of loading is due to the stronger (demagnetizing) dipolar interactions caused by the decrease in the inter-particle distance. Burke et al. [51] also reported a similar decrease in H_C for polymer-coated Fe nanoparticles, where a decrease of 124 Oe was observed as the amount of Fe was increased from 21 to 51 wt.%.

Riquelme et al.[13]reported coercivity values ranging between 500 and 550 Oe for PP magnetic nanocomposites with 2–6 wt.% of CNT-Fe obtained by melt mixing. More recently, Sim et al. [52] have reported on Fe_3O_4@PANI magnetic materials prepared by oxidation polymerization of PANI on the surface of Fe_3O_4. They obtained a coercivity of ~40 Oe, which is a very low value as compared to our results. Santos et al. [53] used polyurethanes, PU/3 and PU/10 wt.% of Fe_3O_4 synthetic talc and obtained coercivities of 275 and 250 Oe at 2K, respectively, which represent values around three times lower than those reported here. Zhu et al. [54] also reported coercivities of 22 Oe for PP nanocomposites filled with 12 wt.% of Fe@Fe_2O_3core@shell nanoparticles at a higher applied field of 90 kOe at room temperature, producing soft ferromagnetic materials. Owing to the high coercivities at room temperature obtained in this work, we can say that they are ferromagnetic materials, in which magnetism can be modulated with the amount of filler.

4. Conclusions

Magnetic and conducting properties are important for the design of new polymeric devices for different applications. The SEM and TEM showed a good dispersion of the filler into the PP matrix, resulting in PP-CNT-Fe nanocomposites with improved thermal stability. The conductivity sharply rises to 7.8×10^{-5} S cm^{-1} with the addition of 3.8 wt.% of CNT-Fe and reaches its highest value of 1.3×10^{-4} S cm^{-1}as the amount of filler increases to 7.5 wt.%. The results show the ferromagnetic nature of the PP with very low percentage of filler at room temperature. This is one of the most remarkable results of this work; our nanocomposites show high coercivities at room temperature, when most works in this area have reported materials with high magnetization only at very low temperatures. This achievement is attributed to the protection of

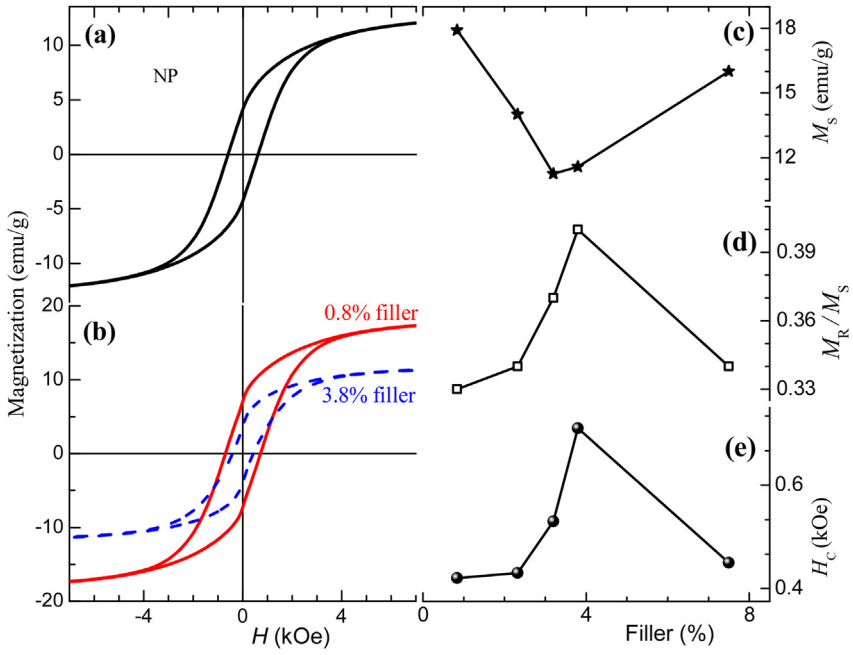

Fig. 4. (a) Room temperature magnetization hysteresis loop of the CNT-Fe powder and (b) representative loops for PP/CNT-Fe nanocomposites. The variations in M_S(c), M_R/M_S (d), and H_C (e) with the filler content are also plotted.

the Fe NPs by CNTs that avoid oxidation and to the good dispersion of the filler in the polymer matrix.

Acknowledgments

The authors are grateful to the TWAS-CNPq for the fellowship to Muhammad Nisar, the CNPq for the special visiting research fellowship to Professor Raúl Quijada, and CNPq grant 302902/2013-9. Professor Raúl Quijada acknowledges the Millennium Nucleus of Chemical Processes and Catalysis (CPC), grant number NC120082, and Dr. Victor Fuenzalida from Laboratorio de Superficies, Departamento de Fisica, Facultad de Cienciasfísicas y Matematicas, Universidad de Chile, for laboratory support. We also thank CME and LRNANO from UFRGS for the microscopy analysis and Dr. Eliana Galland Barrera for the Absorption Atomic analyses. The magnetic characterization was performed in collaboration with the Laboratory of Magnetism at IF-UFRGS.

References

[1] G. Kickbick, Concepts for the incorporation of inorganic building blocks into organic polymers on a nanoscale, Prog. Polym. Sci. 28 (2003) 83–114.
[2] P. Song, Z. Cao, Y. Cai, L. Zhao, Z. Fang, S. Fu, Fabrication of exfoliated graphene based-polypropylene nanocomposites with enhanced mechanical and thermal properties, Polymer 52 (2011) 4001–4020.
[3] S. Iijima, Helical microtubules of graphitic carbon, Nature 354 (1991) 56–58.
[4] P.M. Ajayan, O. Stephan, C. Colliex, D. Trauth, Aligned carbon nanotube arrays formed by cutting a polymer resin-nanotube composite, Science 265 (1994) 1212–1214.
[5] M. Moniruzzaman, K.I. Winey, Polymer nanocomposits containing carbon nanotubes, Macromolecules 39 (2006) 5194–5205.
[6] A.K.T. Lau, D. Hui, The revolutionary creation of new advanced materials—carbon nanotube composites, Compos. Part B 33 (2002) 263–277.
[7] S. Bredeau, S. Peeterbroeck, D. Bonduel, M. Alexandre, P. Dubois, From carbon nanotube coatings to high-performance polymer nanocomposites, Polym. Int. 57 (2008) 547–553.
[8] P. Ajayan, in: H.S. Nalwa (Ed.), Handbook of Nanostructured Materials and Nanotechnology, vol. 5, Academic Press, New York, 2000, pp. 501–575.
[9] A. Funk, W. Kaminsky, Polypropylene carbon nanotubes nanocomposites by *in situ* polymerization, Compos. Sci. Technol. 67 (2007) 906–915.
[10] P. Zapata, R. Quijada, Polypropylene nanocomposites obtained by in situ polymerization using metallocenes catalyst: influence of the nanoparticles on the final polymer morphology, J. Nano. Mater 194543 (2012) 6.
[11] R.S. Aranjo, R.J.B. Oliveira, M.F.V. Marques, Preparation of nanocomposites of polypropylene with carbon nanotubes via masterbatches produced by *in situ* polymerization and by melt extrusion, Macromol. React. Eng 8 (2014) 747–754.
[12] R.J.B. Oliveira, J.S. Santos, M.F.V. Marques, Preparation of Ziegler-Natta catalysts for the synthesis of polypropylene/carbon nanotubes nanocomposites by *in situ* polymerization, Polímeros 24 (2014) 13–19.
[13] J. An, G.Jeon, Y.Jeong, Preparation and properties of polypropylene nanocomposites reinforced with exfoliated graphene, Fibers Polym. 13 (2012) 507–514.
[14] J. Riquelme, C.A. Garzón, C.P. Bergmann, J. Geshev, R. Quijada, Development of multifunctional polymer nanocomposites with carbon-based hybrid nanostructures synthesized from ferrocene, Eur. Polym. J. 75 (2016) 200–209.
[15] P. Potschke, A.R. Bhattacharyy, A. Janke, Carbon nanotubes-filled polycarbonate composites produced by melt mixing and their use in blend with polyethylene, Carbon 42 (2004) 965–969.
[16] W.E. Dondero, R.E. Gorga, Morphological and mechanical properties of carbon nanotube/polymer composites via melt compounding, J. Polym. Sci. Polym. Phys. 44 (2006) 864–878.
[17] S. Curran, A.P. Davey, J. Coleman, A. Dalton, B. McCarthy, S. Maier, Evolution and evaluation of the polymer/nanotube composite, Synth. Met. 103 (1–3) (1999) 2559–2562.
[18] A. Funck, W. Kaminsky, Polypropylene carbon nanotube composites by *in situ* polymerization, Compos. Sci. Technol. 67 (5) (2007) 906–915.
[19] S.H. Lee, E. Cho, S.H. Jeon, J.R. Youn, Rheological and electrical properties of polypropylene composites containing functionalized multi-walled carbon nanotubes and compatibilizers, Carbon 45 (2007) 2810–2822.
[20] M.A. Milani, R. Quijada, N.R.S. Basso, A.P. Graebin, G.B. Galland, influence of the graphite type on the synthesis of polypropylene graphene nanocomposites, J. Polym. Sci. Part A Polym. Chem. 50 (2012) 3598–3605.
[21] J.M.D. Coey, Whither magnetic materials, J. Magn. Magn. Mater. 196–197 (1999) 1–7.
[22] R.D. Shull, L.H. Bennett, Nanocomposite magnetic materials, Nanostruct. Mater. 1 (1992) 83–88.
[23] J. Zhu, S. Wei, M. Chen, H. Gu, S.B. Rapole, S. Pallavkar, T.C. Ho, J. Hopper, Z. Guo, Magnetic nanocomposites for environmental remediation, Adv. Powder. Technol. 24 (2013) 459–467.
[24] S. Kalia, S. Kango, A. Kumar, Y. Haldorai, B. Kumari, S. Kumar, Magnetic polymer nanocomposites for environmental and biomedical applications, Colloid Polym. Sci. 292 (2014) 2025–2052.
[25] S. Wei, Q. Wang, J. Zhu, L. Sun, H. Lin, Z. Guo, Multifunctional composite core–shell nanoparticles, Nanoscale 3 (2011) 4474–4502.
[26] A. Morelos-Gómez, F. Lopez-Urias, E. Munoz-Sandoval, C.L. Dennis, R.D. Shull, H. Terrones, M. Terrones, Controlling high coercivities of ferromagnetic nanowires encapsulated in carbon nanotubes, J. Mater. Chem. 20 (2010) 5906–5914.
[27] C. He, N. Zhao, C. Shi, J. Li, H. Li, Magnetic properties and transmission electron

microscopy studies of Ni nanoparticles encapsulated in carbon nanocages and carbon nanotubes, Mater. Res. Bull. 43 (2008) 2260–2265.
[28] R. Bhatia, V. Prasad, Synthesis of multiwall carbon nanotubes by chemical vapor deposition of ferrocene alone, Solid State Commun. 150 (2010) 311–315.
[29] A.G. Osorio, C.P. Bergmann, Effect of surface area of substrates aiming the optimization of carbon nanotube production from ferrocene, Appl. Surf. Sci. 264 (2013) 794–800.
[30] A.G. Osorio, L.G. Pereira, J.B.M. da Cunha, C.P. Bergmann, Controlling the magnetic response of carbon nanotubes filled with iron-containing material, Mater. Res. Bull. 48 (2013) 4168–4173.
[31] F.C. Fim, J.M. Guterres, N.R.S. Basso, G.B. Galland, Polyethylene/graphite nanocomposites obtained by in situ polymerization, J. Polym. Sci. Part A Polym. Chem. 48 (2010) 692–698.
[32] M.A. Milani, R. Quijada, N.R.S. Basso, A.P. Graebin, G.B. Galland, Influence of the graphite type on the synthesis of polypropylene graphene nanocomposites, Polym. Sci. Part A Polym. Chem. 50 (2012) 3598–3605.
[33] M.A. Milani, D. González, R. Quijada, N.R.S. Basso, M.L. Cerrada, D.S. Azambuja, G.B. Galland, Polypropylene/grapheme nanosheet nanocomposites by in situ polymerization: synthesis, characterization and fundamental properties, Compos. Sci. Technol. 84 (2013) 1–7.
[34] F.C. Fim, N.R.S. Basso, A.P. Graebin, D.S. Azambuja, G.B. Galland, Thermal, electrical, and mechanical properties of polyethylene-graphene nanocomposites obtained by in situ polymerization, J. Appl. Polym. Sci. 128 (2013) 2630–2637.
[35] M.A. Milani, D. González, R. Quijada, R. Benavente, J. Arranz-Andrés, G.B. Galland, Synthesis, characterization and properties of poly(propylene-1-octene)/graphite nanosheet nanocomposites obtained by in situ polymerization, Polymer 65 (2015) 134–142.
[36] G. Pavoski, T. Maraschin, M.A. Milani, D.S. Azambuja, R. Quijada, C.M. Moura, N.R.S. Basso, G.B. Griselda, Polyethylene/reduced graphite oxide nanocomposites with improved morphology and conductivity, Polymer 81 (2015) 79–86.
[37] M. Nisar, C.P. Bergmman, J. Geshev, R. Quijada, G.B. Galland, An efficient approach to the polyethylene magnetic nanocomposites, Polymer 97 (2016) 131–137.
[38] D.E. Park, H.S. Chae, H.J. Choi, A. Maity, Magnetite-polypyrrole core-shell structured microspheres and their dual stimuli-response under electric and magnetic field, J. Mater. Chem. C 3 (2015) 3150–3158.
[39] P. Kim, N.M. Doss, J.P. Tillotson, P.J. Hotchkiss, M.J. Pan, S.R. Marder, J. Li, J.P. Calame, J.W. Perry, High energy density nanocomposites based on surface-modified BaTiO(3) and a ferroelectric polymer, ACS.Nano. 3 (9) (2009) 2581–2592.
[40] Q. Dai, D. Berman, K. Virwani, J. Frommer, P.O. Jubert, M. Lam, T. Topuria, W. Imaino, A. Nelso, Self-assembled ferrimagnet-polymer composites for magnetic recording media, Nano. Lett. 10 (2010) 3216–3221.
[41] T. Shimad, K. Ookubo, N. Komuro, T. Shimizu, N. Uehara, Blue-to-Red chromatic sensor composed of gold nanoparticles conjugated with thermoresponsive copolymer for thiol SensingLangmui 23 (22) (2007) 11225–11232.
[42] Z. Guo, S.E. lee, H. kim, S. Par, H.T. Hahn, A.B. Karki, D.P. Young, Fabrication characterization and microwave properties of polyurethane nanocomposites reinforced with iron oxide and barium titanate nanoparticles, Acta. Mater 57 (1) (2009) 267–277.
[43] M. Resano, E. Bolea-Fernández, E. Mozas, M.R. Flórez, P. Gringberg, R.E. Sturgeon, Simultaneous determination of Co, Fe, Ni and Pb in carbon nanotubes by means of solid sampling high-resolution continuum source graphite furnace atomic absorption spectrometry, J. Anal. At. Spectrom. 28 (2013) 657–665.
[44] S.P. Bao, S.C. Tjong, Mechanical behavior of polypropylene/carbon nanotube nanocomposites: the effect of loading rate and temperature, Mater. Sci. Eng. A 485 (2008) 508–516.
[45] W. Leelapornpisit, M.T. Ton-That, F. Perrin-Sarazin, K.C. Cole, J. Denault, B. Simard, Effect of carbon nanotubes on the crystallization and properties of polypropylene, J. Polym. Sci. Polym. Phys. 43 (2005) 2445–2453.
[46] N.R. Raravikar, L.S. Schadler, A. Vijayaraghavan, Y. Zhao, B. Wei, P.M. Ajayan, Synthesis and characterization of thickness-aligned carbon Nanotube–Polymer composite films, Chem. Mater 17 (2005) 974–983.
[47] B.B. Marosfio, A. Szabo, Gy Marosi, D. Tabuani, G. Camino, S. Pagliari, Thermal and spectroscopic characterization of polypropylene-carbon nanotube composites, J.Therm. Anal.Calorim. 86 (3) (2006) 669–673.
[48] M.H. Al-saleh, Electrical conductivity carbon naotubes/polypropylene nanocomposites with improve mechanical properties, Material Des. 85 (2015) 76–81.
[49] F.F. Fang, Y.D. Liu, H.J. Chio, Y. Seo, Core-shell structure carbonyl iron microspheres prepared via dual-step functionality coatings and their magneto rheological response, ACS. Appl. Mater. Interf. 3 (2011) 3487–3495.
[50] Q. He, T. Yuan, J. Zhu, Z. Luo, N. Haldolaarachchige, L. Sun, A. Khasanov, Y. Li, D.P. Young, S. Wei, Z. Guo, Magnetic high density polyethylene nanocomposites reinforced with in-situ synthesized Fe@FeO core-shell nanoparticles, Polymer 53 (2012) 3642–3652.
[51] N.A.D. Burke, H.D.H. Stover, F.P. Dawson, Preparation and characterization of polymer-coated iron nanoparticles, Chem. Matter 14 (2002) 4752–4761.
[52] B. Sim, H.S. Chea, H.J. Choi, Fabrication of polyaniline coated iron oxide hybrid particles and their dual stimuli-response under electric and magnetic fields, Exp. Polym. Lett. 9 (8) (2015) 736–743.
[53] L.M.D. Santos, R. Ligabue, A. Dumas, C.L. Roux, P. Micoud, J.F. Meunier, F. Martin, S. Einloft, New magnetic nanocomposites: polyurethane/Fe_3O_4 synthetic talc, Eur. Polym. J. 69 (2015) 38–49.
[54] J. Zhu, S. Wei, Y. Li, L. Sun, N. Haldolaarachchige, D.P. Young, C. Southworth, A. Kasanov, Z. Luo, Z. Guo, Surfactant-free synthesized magneticpolypropylene nanocomposites: rheological, electrical, magnetic, and thermal properties, Macromolecules 44 (2011) 4382–4391.